Double-parton scattering effects in D^0B^+ and B^+B^+ meson-meson pair production in proton-proton collisions at the LHC

Rafał Maciuła* and Antoni Szczurek†,‡

Institute of Nuclear Physics, Polish Academy of Sciences, Radzikowskiego 152, PL-31-342 Kraków, Poland

(Received 15 March 2018; published 14 May 2018)

We extend our previous studies of double-parton scattering (DPS) to simultaneous production of $c\bar{c}$ and $b\bar{b}$ and production of two pairs of $b\bar{b}$. The calculation is performed within a factorized ansatz. Each parton scattering is calculated within the k_T-factorization approach. The hadronization is done with the help of fragmentation functions. Production of D mesons in our framework was tested in our previous works. Here, we present our predictions for B mesons. A good agreement is achieved with the LHCb data. We present our results for $c\bar{c}b\bar{b}$ and $b\bar{b}b\bar{b}$ final states. For completeness, we compare results for double- and single-parton scattering (SPS). As for the $c\bar{c}c\bar{c}$ final state, the DPS dominates over the SPS, especially for small transverse momenta. We present several distributions and integrated cross sections with realistic cuts for simultaneous production of D^0B^+ and B^+B^+, suggesting future experimental studies at the LHC.

DOI: 10.1103/PhysRevD.97.094010

I. INTRODUCTION

Phenomena of multiple-parton interaction (MPI) have become very important for precise description of high-energy proton-proton collisions in the ongoing LHC era. There are several experimental and theoretical studies of soft and hard MPI effects in progress (see e.g., Refs. [1,2]), so far mostly concentrated on double-parton scattering (DPS). In many cases, exploration of DPS mechanisms for different processes needs dedicated experimental analysis and is strongly limited because of the large background coming from the standard single-parton scattering (SPS).

Some time ago, we proposed and discussed double open charm meson production $pp \to DDX$ as potentially one of the best reactions to study hard double-parton scattering effects at the LHC [3]. This conclusion was further confirmed by the LHCb Collaboration that has reported surprisingly large cross sections for DD meson-meson pair production in pp-scattering at 7 TeV [4]. As we have shown in our subsequent studies, the LHCb double charm data cannot be explained without the DPS mechanism [5]. In this case, the standard SPS contribution is much smaller and the data sample is clearly dominated by the DPS component [6,7].

Subsequently, we have done similar phenomenological studies for other final states. We identified optimal conditions for exploring DPS effects in $pp \to 4\text{jets}X$ [8,9] as well as in $pp \to D^0 + 2\text{jets}X$ and $pp \to D^0\bar{D}^0 + 2\text{jets}X$ [10] reactions for the ATLAS experiment. Very recently, we have also discussed for the first time possible observation of a triple-parton scattering (TPS) mechanism in triple open charm meson production with the LHCb detector [11]. Some rather general features of double-parton scattering were discussed previously both for $b\bar{b}b\bar{b}$ [12] and $c\bar{c}b\bar{b}$ [13] final states. Here, we extend the discussion by including also the single-parton scattering mechanism for a first time.

In this paper, we wish to present results of phenomenological studies of DPS effects in the case of associated open charm and bottom $pp \to D^0B^+X$ as well as double open bottom $pp \to B^+B^+X$ production. In particular, we will show theoretical predictions of integrated and differential cross sections for different energies that could help to conclude whether and how the DPS effects for these two cases can be observed experimentally by the LHCb/CMS collaborations.

II. A SKETCH OF THE THEORETICAL FORMALISM

A. Single-parton scattering

In Fig. 1, we show a diagrammatic representation of the dominant SPS mechanism for double heavy quark pair production. In particular, in the following, we consider

*rafal.maciula@ifj.edu.pl
†antoni.szczurek@ifj.edu.pl
‡Also at University of Rzeszów, PL-35-959 Rzeszów, Poland.

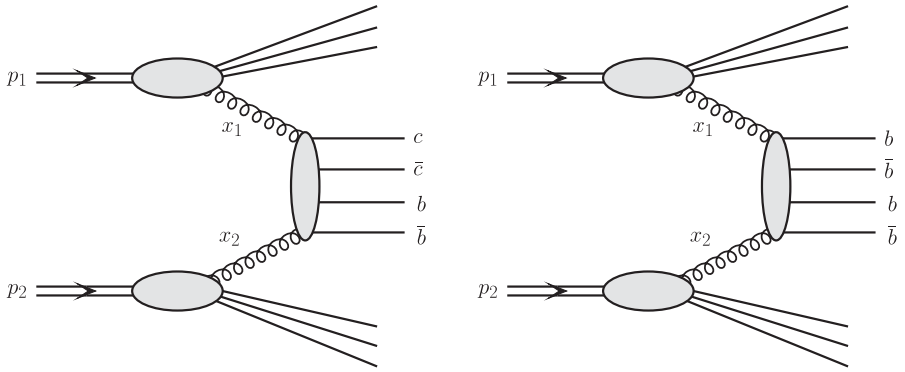

FIG. 1. A diagrammatic representation of the dominant SPS mechanism for the $pp \to c\bar{c}b\bar{b}X$ (left panel) and for the $pp \to b\bar{b}b\bar{b}X$ (right panel) reactions.

mixed $c\bar{c}b\bar{b}$ (left panel) and double bottom $b\bar{b}b\bar{b}$ (right panel) final states; however, here, the production mechanism is the same as was discussed by us in the case of double charm production (see e.g., Ref. [7]).

In the k_T-factorization approach [14–17], the SPS cross section for the $pp \to Q\bar{Q}Q\bar{Q}X$ reaction can be written as

$$d\sigma_{pp\to Q\bar{Q}Q\bar{Q}X} = \int dx_1 \frac{d^2k_{1t}}{\pi} dx_2 \frac{d^2k_{2t}}{\pi} \mathcal{F}_g(x_1, k_{1t}^2, \mu^2) \times \mathcal{F}_g(x_2, k_{2t}^2, \mu^2) d\hat{\sigma}_{gg\to Q\bar{Q}Q\bar{Q}}. \tag{2.1}$$

In the formula above, $\mathcal{F}_g(x, k_t^2, \mu^2)$ is the unintegrated gluon distribution function (uGDF). The uGDF depends on longitudinal momentum fraction x, transverse momentum squared k_t^2 of the gluons entering the hard process, and in general also on a (factorization) scale of the hard process μ^2. The elementary cross section in Eq. (2.1) can be written somewhat formally as

$$d\hat{\sigma}_{gg\to Q\bar{Q}Q\bar{Q}} = \prod_{l=1}^{4} \frac{d^3p_l}{(2\pi)^3 2E_l} (2\pi)^4 \delta^4\left(\sum_{l=1}^{4} p_l - k_1 - k_2\right) \times \frac{1}{\text{flux}} \overline{|\mathcal{M}_{g^*g^*\to Q\bar{Q}Q\bar{Q}}(k_1, k_2)|^2}, \tag{2.2}$$

where E_l and p_l are energies and momenta of final state heavy quarks. Above, only the dependence of the matrix element on the four-vectors of incident partons k_1 and k_2 is made explicit. In general, all four-momenta associated with partonic legs enter. The matrix element takes into account that both gluons entering the hard process are off-shell with virtualities $k_1^2 = -k_{1t}^2$ and $k_2^2 = -k_{2t}^2$. In numerical calculations, we limit ourselves to the dominant gluon-gluon fusion channel of the $2 \to 4$-type parton-level mechanism. We checked numerically that the channel induced by the $q\bar{q}$ annihilation can be safely neglected in the kinematical region under consideration here.

The off-shell matrix elements for higher final state parton multiplicities at the tree level are calculated analytically, applying well-defined Feynman rules [18] or recursive methods, like generalized BCFW recursion [19], or numerically with the help of methods of numerical BCFW recursion [20]. The latter method was already applied for $2 \to 3$ production mechanisms in the case of the $c\bar{c}+$ jet [21] and even for $2 \to 4$ processes in the case of $c\bar{c}c\bar{c}$ [7], four-jet [22], and $c\bar{c}+2$jets [10] final states.

In this paper, we use the same numerical methods. The calculation is performed with the help of KaTie [23], which is a complete Monte Carlo parton-level event generator for hadron scattering processes. It can be applied to any arbitrary processes within the standard model, for several final-state particles, and for any initial partonic state with on-shell or off-shell partons. The scattering amplitudes are calculated numerically as a function of the external four-momenta via the Dyson-Schwinger recursion [24] generalized also to tree-level off-shell amplitudes. The phase-space integration is done with the help of a Monte Carlo program with an adaptive phase-space generator, previously incorporated as a part of the AVHLIB library [25,26].

In the present calculation, we use $\mu^2 = \sum_{i=1}^{4} m_{it}^2/4$ as the renormalization/factorization scale, where m_{it}'s are the transverse masses of the outgoing heavy quarks. We take running α_s at next-to-leading order (NLO), charm quark mass $m_c = 1.5$ GeV, and bottom quark mass $m_b = 4.75$ GeV. The above choices are kept the same also in the case of the double-parton scattering calculation except for the scales. Uncertainties related to the choice of the parameters were discussed very recently in Ref. [10] and will be not considered here. As a default, we use the LO Kimber-Martin-Ryskin (KMR) [27,28] prescription for unintegrated gluon distributions calculated from the MMHT2014nlo PDFs [29]. As was discussed in Ref. [30], the LO KMR model together with NLO PDFs leads to gluon distributions compatible with their counterparts calculated within full NLO KMR approach. In some places, to show possible uncertainties, we also use the JH2013 [31] and Jung setA0 [32] gluon UPDFs that are numerical solutions of the CCFM evolution equation.

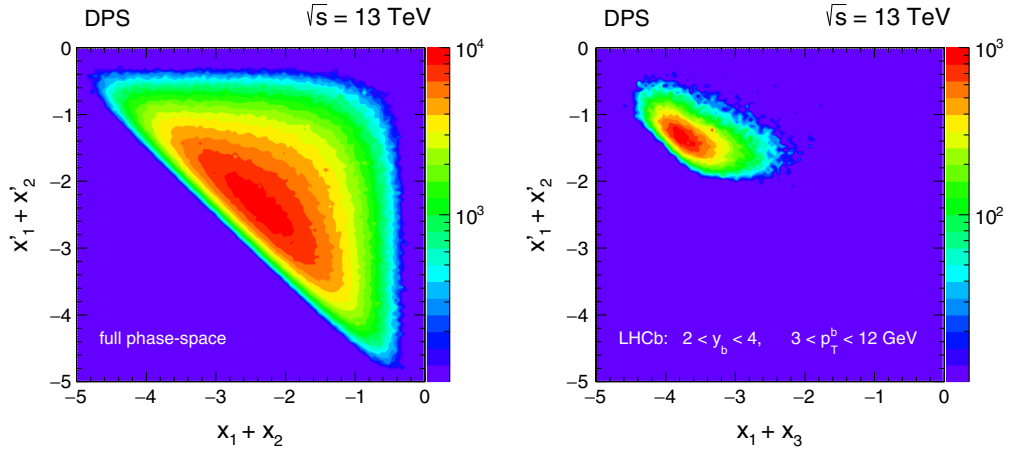

FIG. 2. Double-differential distribution in sum of x's of gluons from one $(x_1 + x_2)$ and second $(x'_1 + x'_2)$ proton for double $b\bar{b}$ production at $\sqrt{s} = 13$ TeV. The left panel shows predictions in the full phase space and the right panel for the relevant LHCb kinematical domain.

The effects of the $c \to D^0$ and $b \to B^+$ hadronization are taken into account via the standard fragmentation function (FF) technique. We use the scale-independent Peterson model of FF [33] with $\varepsilon_c = 0.05$ and $\varepsilon_b = 0.004$, which is commonly used in the literature in the context of heavy quark fragmentation. Details of the fragmentation procedure together with discussion of the uncertainties related to the choice of the FF model can be found e.g., in Ref. [34]. In the last step, the cross section for the meson is normalized by the relevant branching fractions $\mathrm{BR}(c \to D^0) = 0.565$ and $\mathrm{BR}(b \to B^+) = 0.4$.

B. Double-parton scattering

A formal theory of multiple-parton scattering (see e.g., Refs. [35,36]) is rather well established but still not fully applicable for phenomenological studies. In general, the DPS cross sections can be expressed in terms of the double-parton distribution functions (dPDFs). However, the currently available models of the dPDFs are still rather at a preliminary stage. So far they are formulated only for gluon or for valence quarks and only in a leading-order framework which is for sure not sufficient for many processes, especially when heavy quark production is considered.

Instead of the general form, one usually follows the assumption of the factorization of the DPS cross section. Within the factorized ansatz, the dPDFs are taken in the following form,

$$D_{1,2}(x_1, x_2, \mu) = f_1(x_1, \mu) f_2(x_2, \mu) \theta(1 - x_1 - x_2), \quad (2.3)$$

where $D_{1,2}(x_1, x_2, \mu)$ is the dPDF and $f_i(x_i, \mu)$ are the standard single PDFs for the two generic partons in the same proton. The factor $\theta(1 - x_1 - x_2)$ ensures that the sum of the two parton momenta does not exceed 1. It is known that the QCD evolution for collinear double-parton distributions leads to strong suppression of the DPS cross sections at the edges $(x_1 + x_2 \to 1,\ x'_1 + x'_2 \to 1)$ of the phase space [37]. In principle, such a suppression could change predictions for DPS cross sections. In general, the effect should be larger for double $b\bar{b}$ production than for $c\bar{c}b\bar{b}$ production. In Fig. 2, we show a two-dimensional plot of the sum of x's of gluons from the first proton versus similar sum of x's of gluons for the second proton for the $b\bar{b}b\bar{b}$ production. In the left panel, we show the result for the full phase space, while the right panel shows the result when both b quarks (or both $\bar{b}$ antiquarks) are within the LHCb acceptance $(2 < y_b < 4$ and $3 < p_T^b < 12$ GeV) where the situation could be *a priori* more difficult. Our calculation shows that even there the sum of x's is smaller than 0.1, i.e., is far from the kinematical limits. This justifies the use of the factorized ansatz as in the case of the present analysis.

The differential cross section for $pp \to Q\bar{Q}Q\bar{Q}X$ reaction within the DPS mechanism, sketched in Fig. 3, can be then expressed as follows:

$$\frac{d\sigma^{\mathrm{DPS}}(Q\bar{Q}Q\bar{Q})}{d\xi_1 d\xi_2} = \frac{m}{\sigma_{\mathrm{eff}}} \cdot \frac{d\sigma^{\mathrm{SPS}}(gg \to Q\bar{Q})}{d\xi_1} \cdot \frac{\sigma^{\mathrm{SPS}}(gg \to Q\bar{Q})}{d\xi_2}, \quad (2.4)$$

where ξ_1 and ξ_2 stand for generic phase-space kinematical variables for the first and second scattering, respectively. The combinatorial factor m is equal to 1 for $c\bar{c}b\bar{b}$ and 0.5 for the $b\bar{b}b\bar{b}$ case. When integrating over kinematical variables, one recovers the commonly used pocket formula:

$$\sigma^{\mathrm{DPS}}(Q\bar{Q}Q\bar{Q}) = m \cdot \frac{\sigma^{\mathrm{SPS}}(gg \to Q\bar{Q}) \cdot \sigma^{\mathrm{SPS}}(gg \to Q\bar{Q})}{\sigma_{\mathrm{eff}}}. \quad (2.5)$$

The effective cross section σ_{eff} provides normalization of the DPS cross section and can be roughly interpreted as a

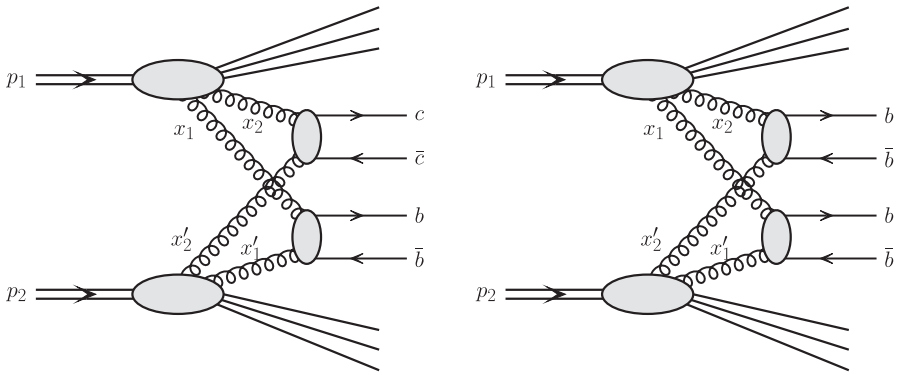

FIG. 3. A diagrammatic representation of the DPS mechanism for the $pp \to c\bar{c}b\bar{b}X$ (left panel) and for the $pp \to b\bar{b}b\bar{b}X$ (right panel) reactions.

measure of the transverse correlation of the two partons inside the hadrons. The longitudinal parton-parton correlations are far less important when the energy of the collision is increased, due to the increase in the parton multiplicity. For small-x partons and for low and intermediate scales, the possible longitudinal correlations can be safely neglected (see e.g., Ref. [38]). In this paper, we use the world-average value of $\sigma_{\rm eff} = 15$ mb provided by several experiments at Tevatron [39–41] and LHC [4,42–45]. Future experiments may verify this value and establish a systematics.

There are several effects that may lead to a violation of the factorized ansatz (2.4), which seems *a priori* a severe approximation. The flavor, spin, and color correlations lead, in principle, to interference effects that result in breaking the pocket-formula (see e.g., Refs. [35,36]). In any case, the spin polarization of the two partons from one hadron can be mutually correlated, especially when the partons are relatively close in phase space (having comparable x's). The two-parton distributions have a nontrivial color structure which also may lead to a non-negligible correlations effects. Such effects are usually not included in phenomenological analyses. They were exceptionally discussed in the context of double charm production [46] but in this case the corresponding effects were found to be very small. Moreover, including perturbative parton splitting mechanism [47–49] and/or imposing sum rules [50] also leads to a breaking of the pocket-formula. However, taken the above and looking forward to further improvements in this field, here we limit ourselves to a more pragmatic approach.

In our present analysis, cross sections for each step of the DPS mechanism are calculated in the k_T-factorization approach, that is:

$$\frac{d\sigma^{\rm SPS}(pp \to Q\bar{Q}X_1)}{dy_1 dy_2 d^2p_{1,t} d^2p_{2,t}} = \frac{1}{16\pi^2 \hat{s}^2} \int \frac{d^2k_{1t}}{\pi} \frac{d^2k_{2t}}{\pi} \overline{|\mathcal{M}_{g^*g^* \to Q\bar{Q}}|^2} \delta^2(\vec{k}_{1t} + \vec{k}_{2t} - \vec{p}_{1t} - \vec{p}_{2t}) \mathcal{F}_g(x_1, k_{1t}^2, \mu^2) \mathcal{F}_g(x_2, k_{2t}^2, \mu^2),$$
$$\frac{d\sigma^{\rm SPS}(pp \to Q\bar{Q}X_2)}{dy_3 dy_4 d^2p_{3,t} d^2p_{4,t}} = \frac{1}{16\pi^2 \hat{s}^2} \int \frac{d^2k_{3t}}{\pi} \frac{d^2k_{4t}}{\pi} \overline{|\mathcal{M}_{g^*g^* \to Q\bar{Q}}|^2} \delta^2(\vec{k}_{3t} + \vec{k}_{4t} - \vec{p}_{3t} - \vec{p}_{4t}) \mathcal{F}_i(x_3, k_{3t}^2, \mu^2) \mathcal{F}_j(x_4, k_{4t}^2, \mu^2). \quad (2.6)$$

The numerical calculations for both SPS mechanisms are also done within the KaTie code, where the relevant fully gauge-invariant off-shell $2 \to 2$ matrix element $\mathcal{M}_{g^*g^* \to Q\bar{Q}}$ is obtained numerically. Its useful analytical form can be found e.g., in Ref. [15]. Here, the strong coupling constant α_S and uGDFs are taken the same as in the case of the calculation of the SPS mechanism. The factorization and renormalization scales for the two single scatterings are $\mu^2 = \frac{m_{1t}^2 + m_{2t}^2}{2}$ for the first, and $\mu^2 = \frac{m_{3t}^2 + m_{4t}^2}{2}$ for the second subprocess.

III. NUMERICAL RESULTS

Let us start this section with a presentation of results of our calculations for inclusive open bottom meson production. In Figs. 4 and 5, we compare our theoretical predictions based on the k_T-factorization approach with the LHCb experimental data [51] at $\sqrt{s} = 7$ TeV. We get a very good agreement with the experimental points for the B^0 meson transverse momentum distributions with the KMR and the Jung setA0 gluon uPDFs. The two sets of JH2013 uPDFs significantly overestimate the low-p_T region. Similar agreement is found for the B^0 meson rapidity distribution, where only the cross section in the lowest rapidity bin $y \in (2.0, 2.5)$ calculated with the KMR uPDFs seems to be slightly overestimated, however the experimental uncertainties in this case are noticeably larger than in other rapidity intervals. Similar high-level agreement between the k_T-factorization predictions and experimental data has been reported by us in the case of inclusive

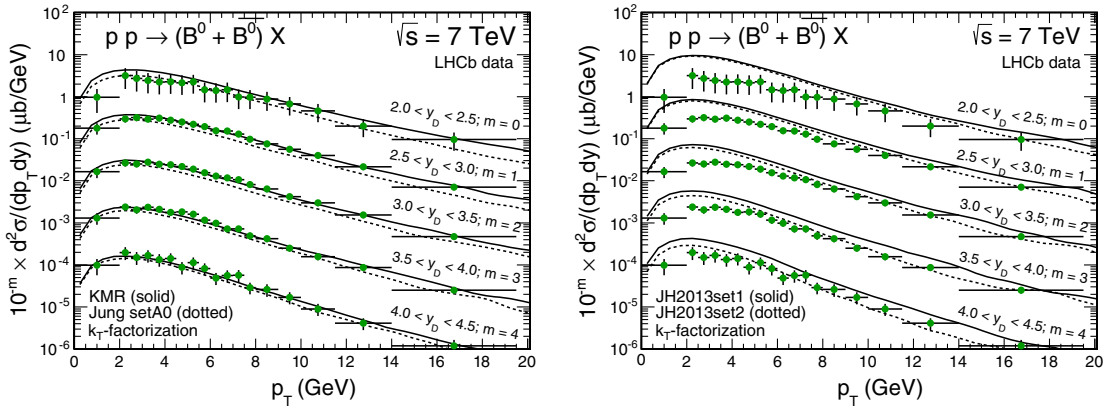

FIG. 4. Transverse momentum distributions of B^0 meson measured by the LHCb experiment at $\sqrt{s} = 7$ TeV [51]. Theoretical predictions are calculated within the k_T-factorization approach. Left and right panel presents results for different uPDFs. Details are specified in the figure.

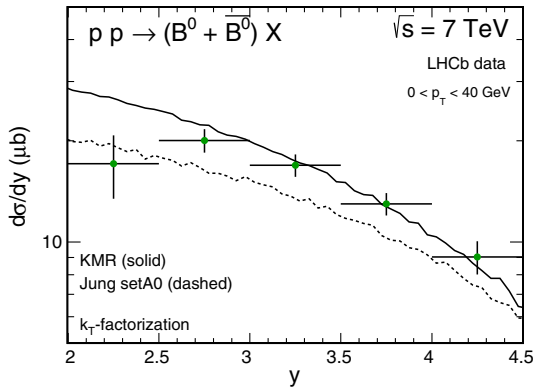

FIG. 5. Rapidity distributions of B^0 meson measured by the LHCb experiment at $\sqrt{s} = 7$ TeV [51]. Theoretical predictions are calculated within the k_T-factorization approach with the KMR (solid line) and the Jung setA0 (dashed line) uPDFs. Details are specified in the figure.

open charm meson production (see e.g., Ref. [52]). This approach was found to be very efficient also for more exclusive correlation observables [34,53]. However, in the case of charm production, only the KMR uPDFs are able to describe the LHC charm data. The CCFM-based uPDFs completely fail [52]. Having those conclusions in mind, we expect that the chosen theoretical framework with the KMR uPDFs should provide a reliable prediction for simultaneous production of charm and bottom as well as for double bottom production via the DPS mechanism. For the later case, reliable predictions can be also obtained with the Jung setA0 gluon uPDFs; however, this statement seems not legitimate in the case of mixed charm-bottom production.

Now we go to the case of simultaneous production of charm and bottom particles. We start with the parton-level predictions for inclusive production of the $c\bar{c}b\bar{b}$ final state at $\sqrt{s} = 13$ TeV. In Fig. 6, we show transverse momentum (top panels) and rapidity (bottom panels) distributions of charm (left panels) and bottom (right panels) quarks. The results are obtained for the full phase space. The SPS (dotted histograms) and DPS (dashed histograms) contributions are shown separately. We observe that the DPS component significantly dominates over the SPS one in the whole rapidity range. It is also true for the transverse momentum distribution of bottom quark. In the case of the charm quark, the situation is slightly different. At small transverse momenta, the DPS mechanism also gives dominant contribution, but both components become comparable when going to larger p_T's.

The optimistic situation for searching for DPS effects in this channel presented above does not change when hadronization effects and kinematical cuts relevant for the LHCb experiment are taken into account. We consider inclusive production of the D^0B^+ pair since this mode has the most advantageous $cb \to DB$ fragmentation probability and leads to the biggest cross sections. In Fig. 7, we show the transverse momentum distribution of D^0 (left panel) and B^+ (right panel) meson at $\sqrt{s} = 13$ TeV for the case of simultaneous D^0B^+-pair production in the LHCb fiducial volume defined as $2 < y < 4$ and $3 < p_T < 12$ GeV for both mesons. Again, the SPS (dotted lines) and the DPS (dashed lines) components are shown separately, together with their sum (solid lines). Here, the conclusions are the same as for the parton-level results. We observe an evident enhancement of the cross section, at the level of order of magnitude, because of the presence of the DPS mechanism in the whole considered kinematical domain. We predict that the D^0B^+ data sample, that could be collected with the LHCb detector, should be DPS dominated in pretty much the same way as in the case of double charm production (see e.g., Ref. [5]).

In Fig. 8, we present correlation observables that could be helpful in experimental identification of the predicted DPS effects. The characteristics of the di-meson invariant mass $M_{D^0B^+}$ (left panel) as well as of the azimuthal angle

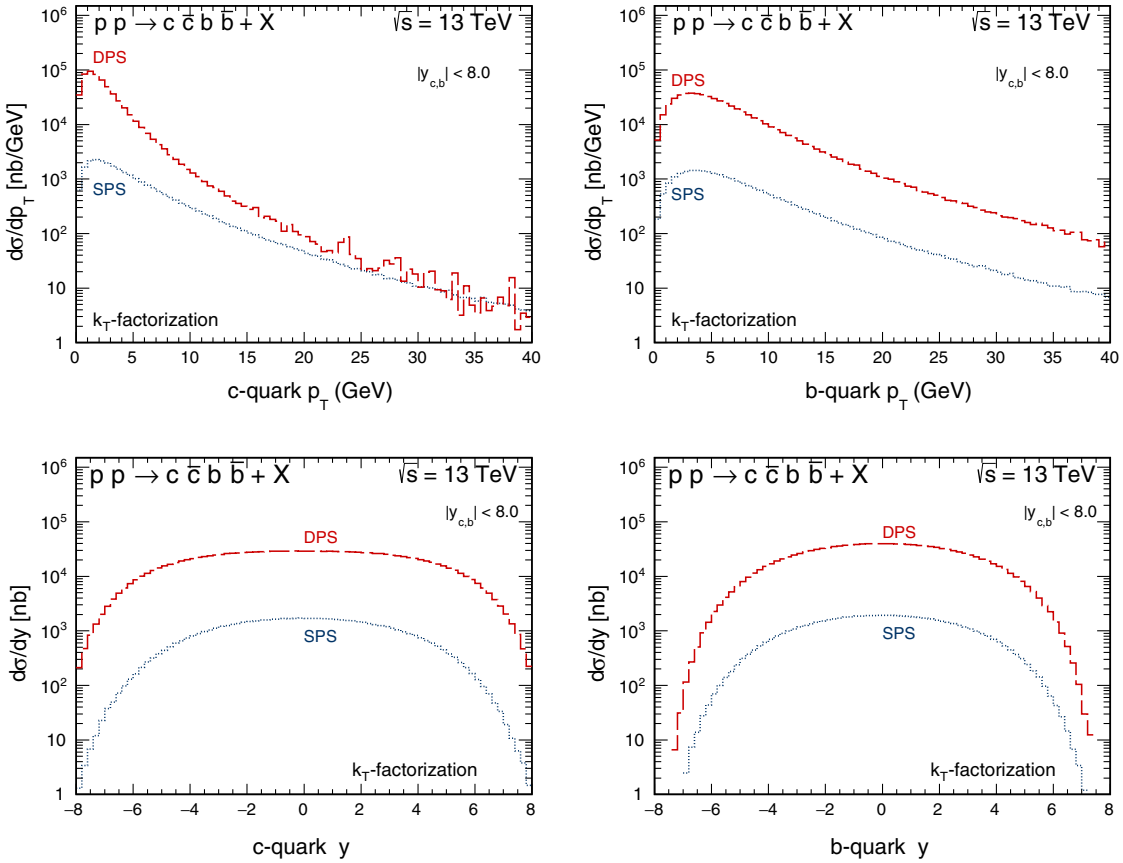

FIG. 6. Transverse momentum (top) and rapidity (bottom) distributions of charm (left) and bottom (right) quark for the case of inclusive production of $c\bar{c}b\bar{b}$ final state. Contributions of the SPS (dotted) and the DPS (dashed) mechanisms are shown separately. The results are obtained within the k_T-factorization approach with the KMR uPDFs for $\sqrt{s} = 13$ TeV.

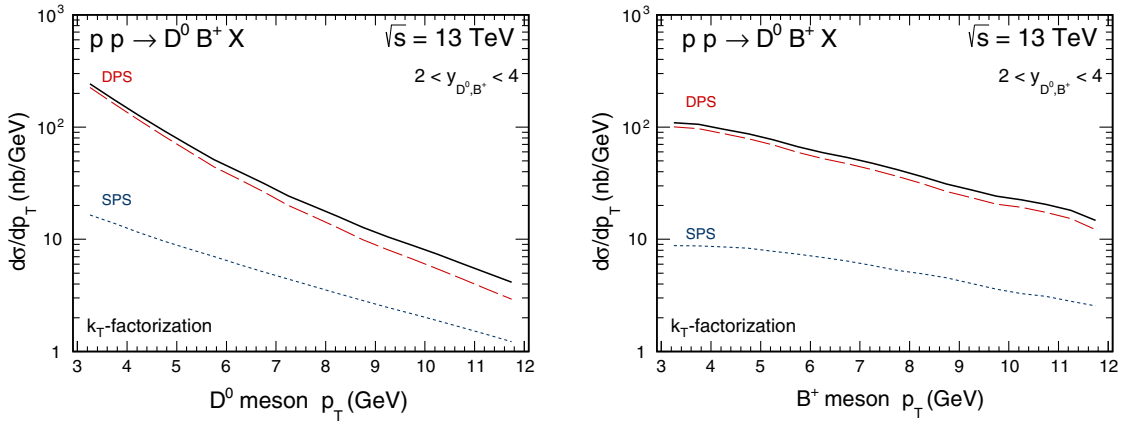

FIG. 7. Transverse momentum distribution of D^0 (left) and B^+ (right) meson at $\sqrt{s} = 13$ TeV for the case of inclusive D^0B^+-pair production in the LHCb fiducial volume. The SPS (dotted) and the DPS (dashed) components are shown separately. The solid lines correspond to the sum of the two mechanisms under consideration. The results are obtained within the k_T-factorization approach with the KMR uPDFs.

$\varphi_{D^0B^+}$ (right panel) differential distributions is clearly determined by the large contribution of the DPS mechanism. We predict a significant enhancement of the cross section at small invariant masses $M_{D^0B^+} \lesssim 15$ GeV and a strong effect of azimuthal angle decorrelation, are related to the DPS mechanism.

Similar conclusions about a possibility of experimental observation and exploration of the DPS effects can be also

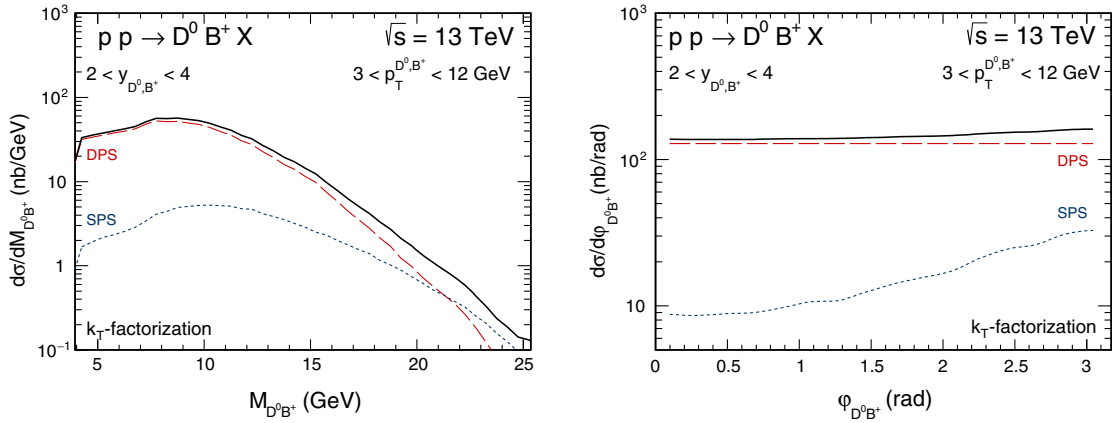

FIG. 8. The same as in Fig. 7 but for the D^0B^+-pair invariant mass (left) and azimuthal angle $\varphi_{D^0B^+}$ (right) distributions.

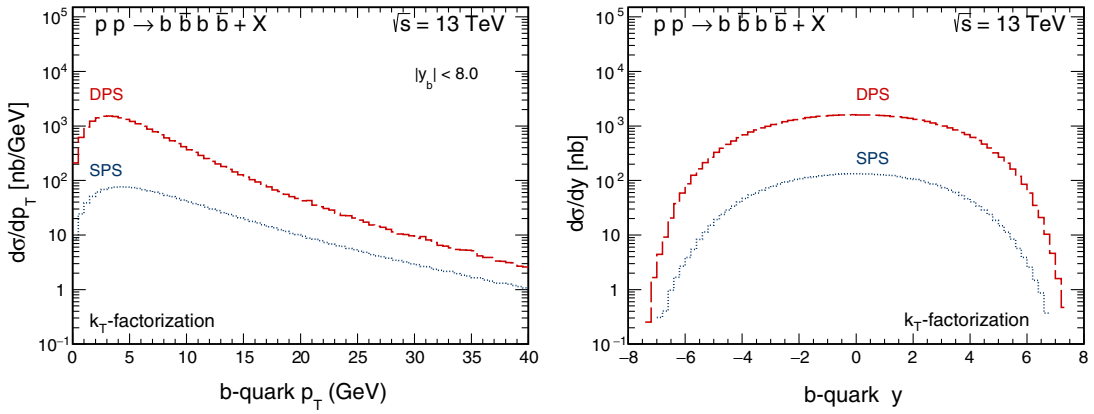

FIG. 9. Transverse momentum (left) and rapidity (right) distributions of bottom quark for the case of inclusive production of $b\bar{b}b\bar{b}$ final state. Contributions of the SPS (dotted) and the DPS (dashed) mechanisms are shown separately. The results are obtained within the k_T-factorization approach with the KMR uPDFs for $\sqrt{s} = 13$ TeV.

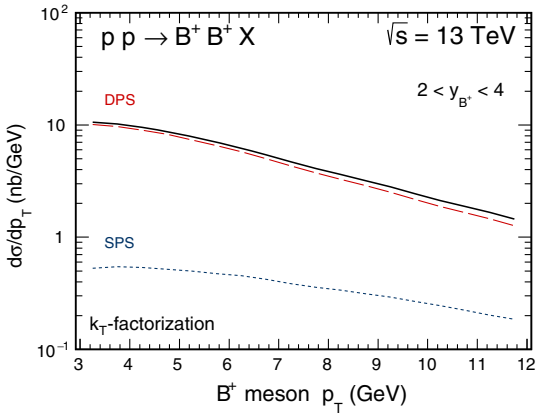

FIG. 10. Transverse momentum distribution of the B^+ meson at $\sqrt{s} = 13$ TeV for the case of inclusive B^+B^+-pair production in the LHCb fiducial volume. The SPS (dotted) and the DPS (dashed) components are shown separately. The solid lines correspond to the sum of the two mechanisms under consideration. The results are obtained within the k_T-factorization approach with the KMR uPDFs.

drawn for the case of double bottom production. As is shown in Fig. 9, the relation between the SPS and the DPS components for the b-quark transverse momentum (left panel) and rapidity (right panel) distribution in the case of $b\bar{b}b\bar{b}$ production is very similar to the relation predicted for the $c\bar{c}b\bar{b}$ final state (see right panels of Fig. 6). The main observed differences are the absolute normalization of the cross section, which is about order of magnitude smaller than in the case of $c\bar{c}b\bar{b}$, and a bit smaller relative contribution of DPS.

The predictions for the B^+B^+ meson-meson pair production for the LHCb experiment only confirm the above statement. The effects related to the DPS mechanism on the B^+-meson transverse momentum (see Fig. 10), on dimeson invariant mass $M_{B^+B^+}$ and on relative azimuthal angle $\varphi_{B^+B^+}$ (see left and right panels of Fig. 11) distributions are pretty much the same as in the case of simultaneous production of the charm and bottom.

In Fig. 12, we show again the B^+B^+-pair invariant mass (left panel) and azimuthal angle $\varphi_{B^+B^+}$ (right panel)

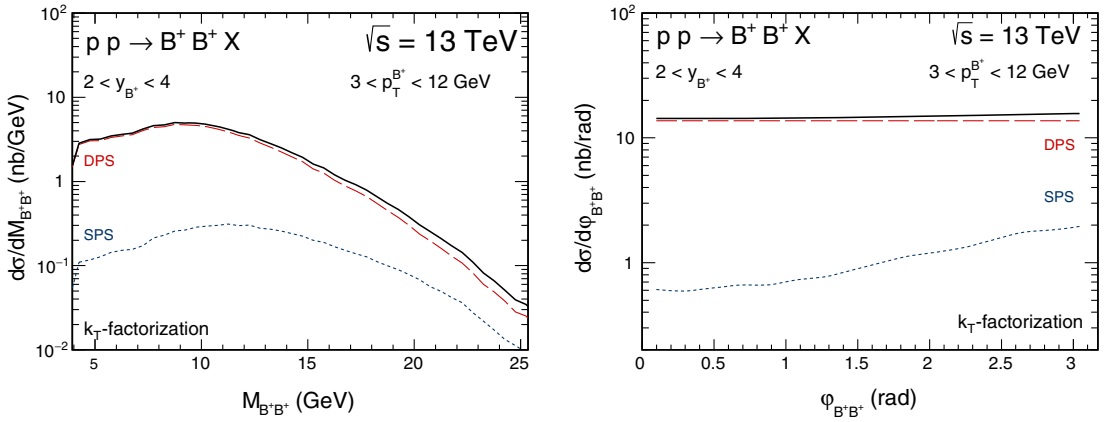

FIG. 11. The same as in Fig. 10 but for the B^+B^+-pair invariant mass (left) and azimuthal angle $\varphi_{B^+B^+}$ (right) distributions.

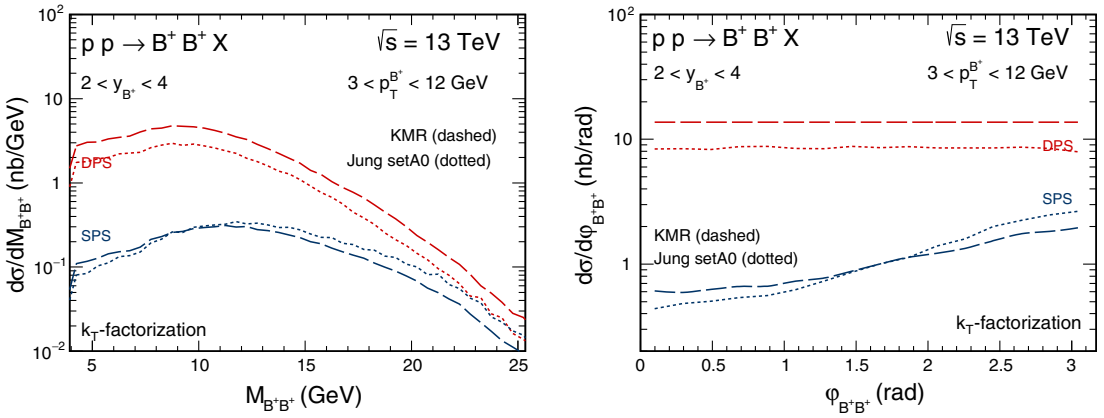

FIG. 12. The B^+B^+-pair invariant mass (left) and azimuthal angle $\varphi_{B^+B^+}$ (right) distributions for the KMR (solid lines) and for the Jung setA0 (dotted lines) uPDFs.

distributions, but this time the default KMR results are compared to the results obtained with the Jung setA0 gluon uPDF. Both models lead to a very similar shape and also normalization of the correlation observables.

To summarize the situation for the LHCb experiment, in Table I, we collect the integrated cross sections for D^0B^+ and B^+B^+ meson-meson pair production in nanobarns within the relevant acceptance: $2 < y_{D^0,B^+} < 4$ and

TABLE I. The integrated cross sections for D^0B^+ and B^+B^+ meson-meson pair production (in nb) within the LHCb acceptance: $2 < y_{D^0,B^+} < 4$ and $3 < p_T^{D^0,B^+} < 12$ GeV, calculated in the k_T-factorization approach. The numbers include the charge conjugate states.

Final state	Mechanism	$\sqrt{s} = 7$ TeV	$\sqrt{s} = 13$ TeV
$D^0B^+ + \bar{D}^0B^-$	DPS	115.50	418.79
	SPS	21.13	51.46
$B^+B^+ + B^-B^-$	DPS	11.04	43.40
	SPS	1.31	3.39

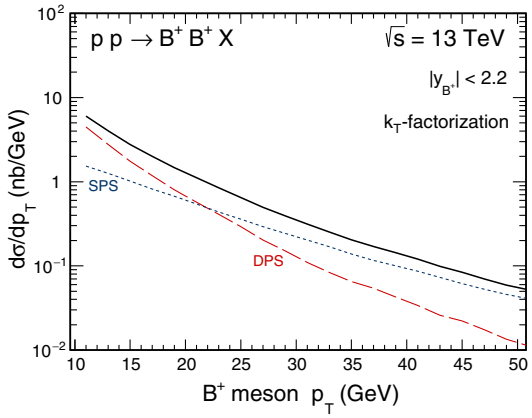

FIG. 13. Transverse momentum distribution of the B^+ meson at $\sqrt{s} = 13$ TeV for the case of inclusive B^+B^+-pair production for the CMS detector acceptance. The SPS (dotted) and the DPS (dashed) components are shown separately. The solid lines correspond to the sum of the two mechanisms under consideration. The results are obtained within the k_T-factorization approach with the KMR uPDFs.

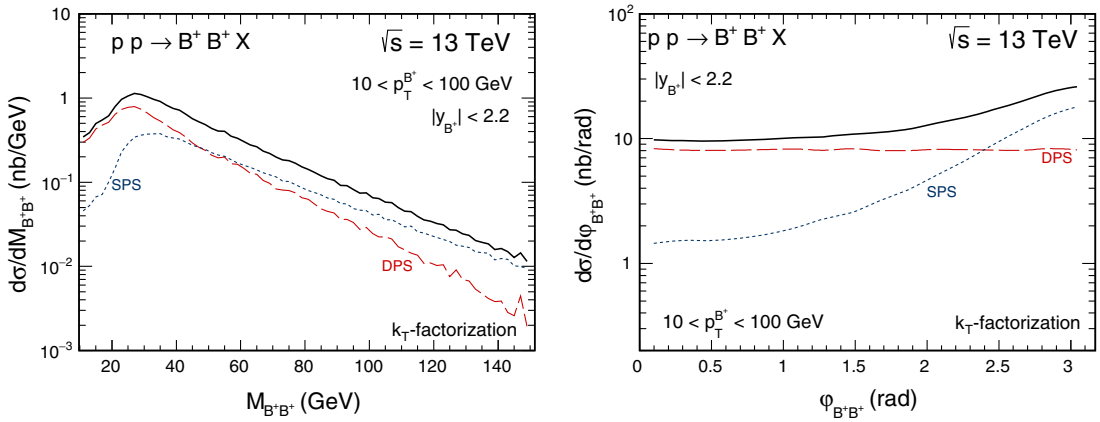

FIG. 14. The same as in Fig. 13 but for the B^+B^+-pair invariant mass (left) and azimuthal angle $\varphi_{B^+B^+}$ (right) distributions.

$3 < p_T^{D^0,B^+} < 12$ GeV. We predict quite large cross sections; in particular, at $\sqrt{s} = 7$ TeV, the calculated cross section for D^0B^+ pair production is only 5 times smaller than the cross section already measured by the LHCb for the D^0D^0 final state [4]. The cross sections for B^+B^+ are an order of magnitude smaller than in the mixed charm-bottom mode; however, they still seem measurable. In both cases, the DPS component is the dominant one. The relative DPS contribution for both energies and for both experimental modes is at the very high level of 90%. This makes the possible measurements very interesting from the point of view of the multiparton interaction community.

Now we wish to present results of similar studies as presented above but for the CMS experiment. Here, the situation may be quite different than in the case of the LHCb experiment because of the quite different kinematical domains defined by the detector acceptance in both experiments. The CMS experiment could collect the data for double bottom production in the region of $|y_{B^\pm}| < 2.2$ and $10 < p_T^{B^\pm} < 100$ GeV. Here, crucial is the lower cut on meson transverse momenta which is quite large (much larger than in the case of the LHCb). This may lead to damping of the relative DPS contribution to the cross section under consideration.

In Fig. 13, we show the differential cross section as a function of the transverse momentum of the B^+ meson for the CMS experiment at $\sqrt{s} = 13$ TeV. Here, the DPS mechanism dominates over the SPS one in the region of small transverse momenta $p_T^{B^+} \lesssim 20$ GeV; however, the effect is not as strong as in the case of the LHCb experiment.

In Fig. 14, we show the relevant distributions in dimeson invariant mass $M_{B^+B^+}$ (left panel) and azimuthal angle $\varphi_{B^+B^+}$ (right panel). We observe a small effect of the enhancement of the cross section especially at small invariant masses $M_{B^+B^+} \lesssim 50$ GeV, related to the DPS mechanism. The azimuthal angle $\varphi_{B^+B^+}$ distribution may be the most helpful for experimental identification of the DPS component within the CMS detector, since we also predict in this case a significant decorrelation of the distribution.

Finally, in Table II, we show predictions for the integrated cross section. The calculated cross sections for B^+B^+ production are very similar to those obtained for the LHCb detector, however, the relative DPS contribution for the CMS experiment is predicted at the level of 50% and 60% at $\sqrt{s} = 7$ and 13 TeV, respectively, i.e., smaller than in the case of LHCb.

TABLE II. The integrated cross sections for B^+B^+ meson-meson pair production (in nb) within the CMS acceptance: $|y_{B^\pm}| < 2.2$ and $10 < p_T^{B^\pm} < 100$ GeV, calculated in the k_T-factorization approach. The numbers include the charge conjugate states.

Final state	Mechanism	$\sqrt{s} = 7$ TeV	$\sqrt{s} = 13$ TeV
$B^+B^+ + B^-B^-$	DPS	6.84	26.27
	SPS	7.24	17.05

IV. CONCLUSIONS

In our previous studies, we discussed in detail the production of $c\bar{c}c\bar{c}$ and $c\bar{c} + 2$ jets final states in order to test and explore double-parton scattering effects. In general, the processes with charm production and/or jets with small transverse momenta have large contribution of double-parton scatterings. Here, we have tried to complete the first stage of exploration of DPS effects in the heavy flavor sector.

In the present paper, we have extended our previous studies to simultaneous production of $c\bar{c}$ and $b\bar{b}$ and two pairs of $b\bar{b}$. It was our aim to understand the interplay of single- and double-scattering processes. The calculations have been done within the standard, thus far, factorized ansatz with two independent partonic scatterings. The so-called $\sigma_{\rm eff}$ parameters have been fixed at the same values as used in our previous studies for double charm production.

The cross section for each step has been calculated within the k_T-factorization approach including transverse momenta of gluons entering hard process. As a default, we have used the Kimber-Martin-Ryskin unintegrated gluon distributions that turned out to be so successful for production of the charm. For $b\bar{b}$ production, we have used also the JH2013 and Jung setA0 unintegrated gluon distributions. The KMR and the Jung setA0 gluon uPDFs provide a similar quality description of the LHCb experimental data for inclusive B meson production. The hadronization of the c quarks to D and b quarks to B mesons have been done with the help of phenomenological fragmentation functions. The Peterson fragmentation functions have been used. We have obtained a good description of the LHCb data for the $B^0 + \bar{B}^0$ production with our standard choice of factorization/renormalization scales.

Having shown that inclusive B meson transverse momentum distributions are rather well understood,[1] we have used our technique to calculate double-parton scattering processes. The calculation of double-parton scattering has been supplemented by calculation of single-parton scattering ($2 \to 4$) processes using codes for automated calculations of the off-shell matrix elements, i.e., including transverse momenta of initial gluons.

First, we explored several different differential distributions for $c\bar{c}b\bar{b}$ and $b\bar{b}b\bar{b}$ production for the whole phase space. We observed clear dominance of the DPS over SPS for small transverse momenta of c or $\bar{c}$ and in the broad range of transverse momenta of b or $\bar{b}$.

Next, we considered distributions for simultaneous production of charmed and bottom mesons. The DPS mechanism has been shown to dominate for small invariant masses of the DB systems. We predicted only a small decorrelation in relative azimuthal angle, typical for DPS dominance.

The situation for $b\bar{b}b\bar{b}$ and two B^+B^+ meson production is rather similar as for the mixed heavy flavor production, but here the dominance of the DPS over SPS is limited to smaller corners of the phase space. A good description of future data will therefore require us to include both DPS and SPS mechanisms simultaneously. All the considered reactions should be easily measured as the corresponding cross sections are rather large. We have obtained similar distributions from the KMR and the Jung setA0 gluon uPDFs.

A comment on the possible, in principle, measurements is in order. Usually experimental subgroups specialize exclusively either in the production of D mesons or B mesons; simultaneous production of D and B mesons will require some coordination of the action of such different subgroups. In our opinion, it would be a valuable effort. An experimental extraction of the $\sigma_{\rm eff}$ parameter for different reactions and a comparison for different processes studied here and in our previous papers would be a simple but necessary step to better understand double scattering in a more precise way. Also a compilation of the $\sigma_{\rm eff}$ would be important phenomenological knowledge. The factorized ansatz is an approximation, and possible deviations from it were discussed in the literature. Once such studies as discussed here are completed, one can try to explore deviations from the simple approach. No clear deviations have been found so far. The only exception is that production of quarkonia pairs with very small values of $\sigma_{\rm eff}$ were extracted from experimental data. The situation in quarkonia pair production is, however, more complex. As discussed recently in Ref. [54], there are several single-parton mechanisms with DPS characteristics. Such processes were not considered so far in theoretical calculations, so the extraction of $\sigma_{\rm eff}$ for these reactions is not reliable. Therefore, in DPS studies, one should concentrate first on processes with heavy quark/meson production.

[1]The same was shown previously for D mesons.

ACKNOWLEDGMENTS

This study was partially supported by the Polish National Science Center Grant No. DEC-2014/15/B/ST2/02528 and by the Center for Innovation and Transfer of Natural Sciences and Engineering Knowledge in Rzeszów.

[1] R. Astalos *et al.*, arXiv:1506.05829.
[2] H. Jung, D. Treleani, M. Strikman, and N. van Buuren, *Proceedings, 7th International Workshop on Multiple Partonic Interactions at the LHC (MPI@LHC 2015): Miramare, Trieste, Italy, 2015*, DESY-PROC-2016-01.
[3] M. Łuszczak, R. Maciuła, and A. Szczurek, Phys. Rev. D **85**, 094034 (2012).
[4] R. Aaij *et al.* (LHCb Collaboration), J. High Energy Phys. 06 (2012) 141; 03 (2014) 108.
[5] R. Maciuła and A. Szczurek, Phys. Rev. D **87**, 074039 (2013).
[6] A. van Hameren, R. Maciuła, and A. Szczurek, Phys. Rev. D **89**, 094019 (2014).
[7] A. van Hameren, R. Maciuła, and A. Szczurek, Phys. Lett. B **748**, 167 (2015).
[8] R. Maciuła and A. Szczurek, Phys. Lett. B **749**, 57 (2015).
[9] K. Kutak, R. Maciuła, M. Serino, A. Szczurek, and A. van Hameren, Phys. Rev. D **94**, 014019 (2016).

[10] R. Maciuła and A. Szczurek, Phys. Rev. D **96**, 074013 (2017).
[11] R. Maciuła and A. Szczurek, Phys. Lett. B **772**, 849 (2017).
[12] A. Del Fabbro and D. Treleani, Phys. Rev. D **66**, 074012 (2002).
[13] E. R. Cazaroto, V. P. Goncalves, and F. S. Navarra, Phys. Rev. D **88**, 034005 (2013).
[14] S. Catani, M. Ciafaloni, and F. Hautmann, Phys. Lett. B **242**, 97 (1990).
[15] S. Catani, M. Ciafaloni, and F. Hautmann, Nucl. Phys. **B366**, 135 (1991).
[16] J. C. Collins and R. K. Ellis, Nucl. Phys. **B360**, 3 (1991).
[17] L. V. Gribov, E. M. Levin, and M. G. Ryskin, Phys. Rep. **100**, 1 (1983).
[18] A. van Hameren, P. Kotko, and K. Kutak, J. High Energy Phys. 01 (2013) 078.
[19] A. van Hameren, J. High Energy Phys. 07 (2014) 138.
[20] M. Bury and A. van Hameren, Comput. Phys. Commun. **196**, 592 (2015).
[21] R. Maciuła and A. Szczurek, Phys. Rev. D **94**, 114037 (2016).
[22] K. Kutak, R. Maciuła, M. Serino, A. Szczurek, and A. van Hameren, J. High Energy Phys. 04 (2016) 175.
[23] A. van Hameren, Comput. Phys. Commun. **224**, 371 (2018).
[24] F. Caravaglios and M. Moretti, Phys. Lett. B **358**, 332 (1995).
[25] A. van Hameren, Acta Phys. Pol. B **40**, 259 (2009).
[26] A. van Hameren, arXiv:1003.4953.
[27] M. A. Kimber, A. D. Martin, and M. G. Ryskin, Phys. Rev. D **63**, 114027 (2001).
[28] G. Watt, A. D. Martin, and M. G. Ryskin, Phys. Rev. D **70**, 014012 (2004); **70**, 079902(E) (2004).
[29] L. A. Harland-Lang, A. D. Martin, P. Motylinski, and R. S. Thorne, Eur. Phys. J. C **75**, 204 (2015).
[30] A. D. Martin, M. G. Ryskin, and G. Watt, Eur. Phys. J. C **66**, 163 (2010).
[31] F. Hautmann and H. Jung, Nucl. Phys. **B883**, 1 (2014).
[32] H. Jung, arXiv:0411287.
[33] C. Peterson, D. Schlatter, I. Schmitt, and P. M. Zerwas, Phys. Rev. D **27**, 105 (1983).
[34] R. Maciuła and A. Szczurek, Phys. Rev. D **87**, 094022 (2013).
[35] M. Diehl and A. Schafer, Phys. Lett. B **698**, 389 (2011).
[36] M. Diehl, D. Ostermeier, and A. Schafer, J. High Energy Phys. 03 (2012) 089; 03 (2016) 001.
[37] V. L. Korotkikh and A. M. Snigirev, Phys. Lett. B **594**, 171 (2004).
[38] J. R. Gaunt and W. J. Stirling, J. High Energy Phys. 03 (2010) 005.
[39] F. Abe *et al.* (CDF Collaboration), Phys. Rev. Lett. **79**, 584 (1997).
[40] F. Abe *et al.* (CDF Collaboration), Phys. Rev. D **56**, 3811 (1997).
[41] V. M. Abazov *et al.* (D0 Collaboration), Phys. Rev. D **81**, 052012 (2010).
[42] G. Aad *et al.* (ATLAS Collaboration), New J. Phys. **15**, 033038 (2013).
[43] S. Chatrchyan *et al.* (CMS Collaboration), J. High Energy Phys. 03 (2014) 032.
[44] G. Aad *et al.* (ATLAS Collaboration), J. High Energy Phys. 04 (2014) 172.
[45] M. Aaboud *et al.* (ATLAS Collaboration), J. High Energy Phys. 11 (2016) 110.
[46] M. G. Echevarria, T. Kasemets, P. J. Mulders, and C. Pisano, J. High Energy Phys. 04 (2015) 034.
[47] M. G. Ryskin and A. M. Snigirev, Phys. Rev. D **83**, 114047 (2011).
[48] J. R. Gaunt, J. High Energy Phys. 01 (2013) 042.
[49] J. R. Gaunt, R. Maciuła, and A. Szczurek, Phys. Rev. D **90**, 054017 (2014).
[50] K. Golec-Biernat, E. Lewandowska, M. Serino, Z. Snyder, and A. M. Stasto, Phys. Lett. B **750**, 559 (2015).
[51] R. Aaij *et al.* (LHCb Collaboration), J. High Energy Phys. 08 (2013) 117.
[52] R. Maciuła, V. A. Saleev, A. V. Shipilova, and A. Szczurek, Phys. Lett. B **758**, 458 (2016).
[53] A. Karpishkov, V. Saleev, and A. Shipilova, Phys. Rev. D **94**, 114012 (2016).
[54] A. Cisek, W. Schäfer, and A. Szczurek, arXiv:1711.07366.